Journal of Sound and Vibration (2001) **243**(2), 347–359
doi:10.1006/jsvi.2000.3417, available online at http://www.idealibrary.com on IDEAL®

ON THE APPLICATION OF SHUNTED PIEZOCERAMICS FOR INCREASING ACOUSTIC TRANSMISSION LOSS IN STRUCTURES

M. Ahmadian and K. M. Jeric

Advanced Vehicle Dynamics Laboratory, Department of Mechanical Engineering, Virginia Tech, MC-0238, *Blacksburg, VA* 24061, *U.S.A. E-mail: ahmadian@vt.edu*

(*Received* 11 *February* 2000, *and in final form* 7 *November* 2000)

The application of electrically shunted piezoceramic materials (PZTs) for increasing transmission loss is studied. A test setup in an SAE J1400 facility is used to analyze the sound transmission loss due to a test plate with shunted PZTs, and to compare the results with an undamped plate and a plate with constrained-layer damping materials. The test results indicate that shunted PZTs can increase sound transmission loss by approximately 6 dB for a pure tone input at 162 Hz, and 7 dB for a broad band input of 10–10 000 Hz. The test results further show that, compared to the constrained layer damping materials that are commonly used in the automotive industry, PZTs provide a substantially higher sound transmission loss-to-weight ratio. This paper will present the test setup in an SAE J1400 facility, the installation of the PZTs on a test plate, and the tuning procedure that is used for the shunt circuits. It also provides a detailed analysis of the results of sound transmission tests for three different test plates, namely an undamped plate, a plate with constrained layer damping, and a plate with electrically shunted PZTs.

1. INTRODUCTION

Piezoceramic materials (PZTs) exhibit a piezoelectric effect, which occurs naturally in quartz crystals, but can be induced in other materials such as specially formulated ceramics consisting mainly of lead, zirconium, and titanium (PZT). The piezoelectric effect provides the ability to use these materials as both sensors and actuators. Piezoceramics can also be used for structural damping because of their ability to efficiently transform mechanical energy to electrical energy and *vice versa*. When PZT elements are used in conjunction with an electrical shunt circuit (commonly called "shunted PZTs") for vibration suppression, the force from the vibration strains the PZT, which generates a voltage difference or electrical energy. This electrical energy can then be dissipated through a resistive circuit [1]. For example, shunted PZTs have already been proven to work effectively in commercial products such as K2 skis. In K2 skis, an imbedded resistor and capacitor (RC) shunt circuit is used to dissipate the vibration energy in the skis and reduce tip flapping [2].

The application of PZTs with different control configurations (such as active control, shunted control, etc.) for reducing vibrations and structure-borne noise has been studied by many researchers in the past few years [3–8]. Almost all of the studies have involved the implementation of an active control system for reducing acoustic radiation from a vibrating structure, also referred to as structure-borne noise. Sun *et al.* [9] used piezoelectric actuators to reduce the structural vibrations and interior noise of a uniform cylindrical shell that models a fuselage section. Two distributed piezoelectric

0022-460X/01/220347 + 13 $35.00/0

actuators were developed based upon the understanding of structural–acoustic coupling properties of the system.

Control of sound radiation from a plate in an acoustic cavity using smart materials was investigated by Shields *et al.* [10]. They applied a patch of active piezoelectric damping composites to the center of a 29·8-cm-square plate made of thin aluminum. The patch was made of PZT fibers embedded in resin. Using a derivative feedback controller, they obtained a 70% attenuation of vibration and sound pressure levels. Active control of sound radiating from a plate was also demonstrated by Varadan *et al.* [11] on a thin square metal plate. The structural vibrations of the plate responsible for the sound/noise radiation were actively controlled with piezoelectric sensors and actuators. This effective method of active noise control was demonstrated for the interior noise of a cabin enclosure by Varadan *et al.* [12]. They used discrete piezoelectric actuators and sensors for the active vibration control of the walls of the enclosure. They were able to achieve significant global noise reduction within the cavity for the dominant modes of the radiation panel.

Lecce *et al.* [13] demonstrated vibration active control in a vehicle by using piezoelectric sensors and actuators. The active structural acoustic control was developed by integrating piezoceramic materials as sensors and actuators into the structural elements of the vehicle. A system with simple feed forward control was implemented to control the floor panel vibrations, and reduce structure-borne noise inside the vehicle.

In addition to the above studies, there exist a limited number of studies that address the use of actively controlled piezoceramics for increasing sound transmission loss through a panel. Henrioulle *et al.* [14] added a flexible honeycomb structure with a piezoelectric PVDF (polyvinylidene fluoride) layer to a double panel partition. With active control of the PVDF, they were able to increase the transmission loss by 10 dB at frequencies below 400 Hz. Xiaoqi *et al.* [15] used active control with piezoelectric actuators and sensors to increase the transmission loss through a thin aluminum plate. The plate was actively controlled at the resonance frequencies of the passive plate where the isolation performance was poor. With one sensor and one actuator, a global sound reduction of 15–22 dB was achieved at the first three resonance frequencies.

As stated earlier, the vast majority of the PZT studies concentrate on the use of actively controlled PZTs for reducing vibrations and the resulting structure-borne noise. This study will attempt to extend the previous PZT studies by examining the application of shunted PZTs for increasing sound transmission loss through a structure. Shunted PZTs are considered here because they offer a simpler and more cost-effective alternative to actively controlled PZTs; therefore, making them more suitable for cost-sensitive applications.

First, the test setup in an SAE J1400 test facility is described followed by a detailed description of the shunt circuit and tuning procedure. Next, the effect of shunted PZTs on increasing sound transmission loss for a test plate with different damping conditions is presented. The test results indicate that shunted PZTs are quite effective in increasing sound transmission loss, without adding any substantial amount of weight to the structure, as compared to the conventional constrained layer damping materials.

2. TEST SETUP

The tests were conducted at an SAE J1400 facility for transmission loss test according to standardized test specifications [16]. The transmission loss test facility has two adjacent rooms, a reverberation room and a semi-anechoic reception room. Panels are placed for testing on a window located between the two rooms. Sound is generated in the reverberation room and the amount of sound transmitted through the window is measured.

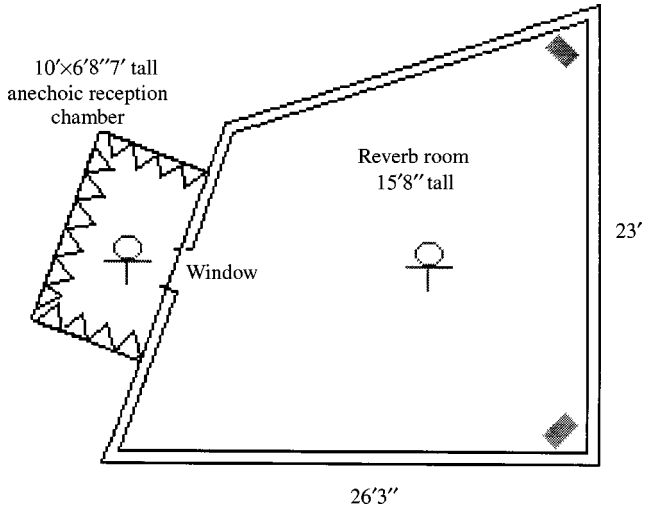

Figure 1. Floor plan of transmission loss test facility. ⚲, Microphone; ■, Speaker.

The SAE J1400 test facility shown in Figure 1 consists of 300-m^3 reverberation room, a semi-anechoic reception chamber, and a joining wall.

For testing, a panel with a variety of different damping materials is inserted in a window located in the joining wall. The window, originally adapted for a 3 ft × 3 ft test panel, had to be modified to accommodate the smaller 600 mm × 500 mm standard test plate.

Initial tests were run with this window in order to calibrate the data acquisition program that measures the noise reduction and calculates the panel transmission loss. Once the test setup was calibrated, transmission loss tests were conducted for the following three test plates: (1) undamped plate, (2) plate with electrically shunted PZTs, (3) plate with constrained layer damping.

Plate 1 is the standard test plate used for establishing the baseline vibration and acoustics results. Plate 2 is the PZT plate with the shunt circuits, and plate 3 is the plate with constrained layer damping material. The purpose for testing plate 3 was to compare the benefits of shunted PZTs with conventional constrained layer damping materials.

3. TEST PLATE CONFIGURATION

Three structurally identical test plates were selected for this study, where each test plate was made of 20-gauge (nominally 1·00 or 0·0396 mm in thickness) galvanized steel and had a test area of 400 mm × 500 mm. This test plate configuration was selected because it is commonly accepted in the automotive industry as the "standard" plate for evaluating noise and vibration effectiveness of various damping materials in the laboratory. The test plates were clamped into place with 14 bolts tightened to a torque of 25 N m, as shown in Figure 2. The bolts were always tightened in the same criss-cross pattern, similar to that for lug nuts on a car wheel, to increase the repeatability of the plate boundary conditions.

Three PZT patches were attached (glued) to the test plate at the locations shown in Figure 3. The location of the PZTs was selected based on an extensive finite element and modal analysis testing that is described in detail in reference [17]. The PZTs were acquired from Piezo Systems, Inc., part number T105-H4E-602. The size of each PZT patch was 72·5 mm × 72·5 mm (2·85 in × 2·85 in) with a thickness of 0·127 mm (0·005 in). The PZTs had

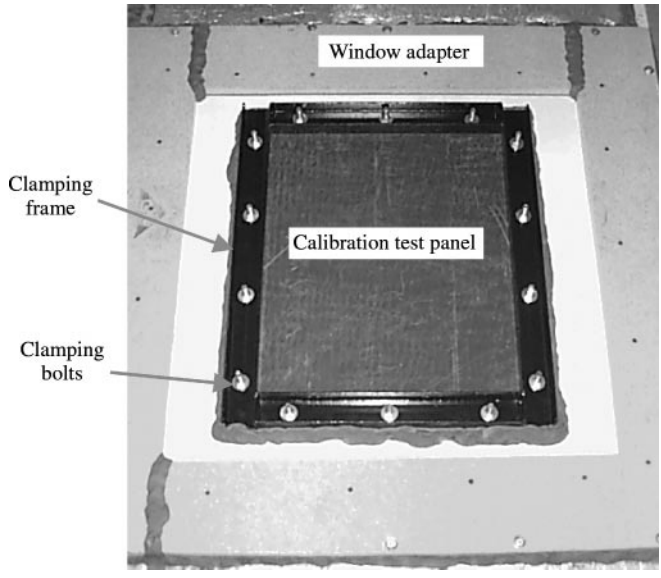

Figure 2. Modified test window with barrier material for calibration test.

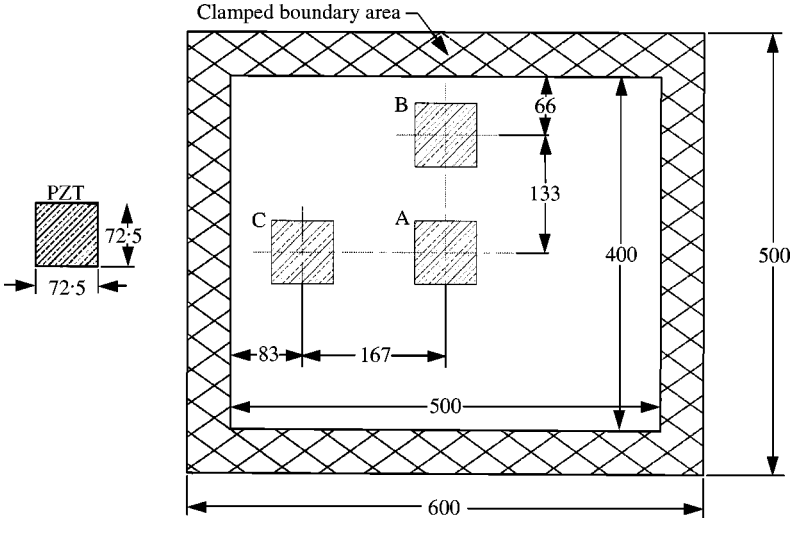

Figure 3. PZT placement on the test plate. Three PZT patches are placed on the test plate, one at the center and the other two along the major and minor axes of the plate. Dimensions are in millimeters.

a relative dielectric constant of 3800 at 1 kHz, and a strain coefficients of $d_{33} = 650\text{E-}12$ m/v and $d_{31} = -320\text{E-}12$ m/v.

4. SHUNT CIRCUIT DESIGN

The shunt circuit chosen for this application was an RLC circuit, similar to the one demonstrated by Hagood and von Flotow [6]. Although other shunting concepts exist, this

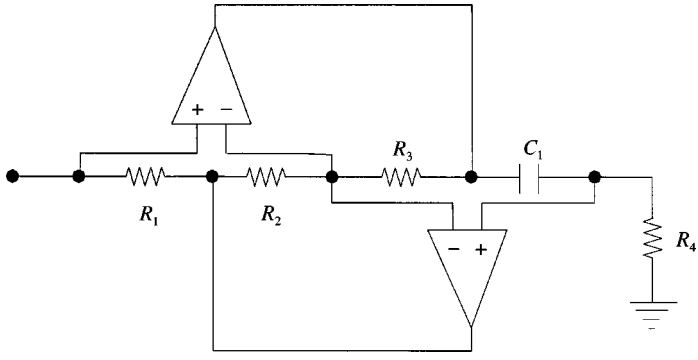

Figure 4. Operational amplifier circuit emulating a variable inductance.

shunt circuit was chosen because it had successfully been used for other applications [18, 19]. The basic resonant shunt design consists of a resistor, an inductor, and a capacitor. The resistor in the circuit is referred to as the load resistor, because it is the mechanism for dissipating the electrical energy. The resistance of the load resistor ranges from 0 to 14 000 Ω, and dissipates approximately 0·002 W of energy from the plate at the resonant peaks. The electrical resonance of the circuit is determined by the value of the inductance and the capacitance, according to

$$\omega_e = \frac{1}{\sqrt{L_s Cpi}}. \tag{1}$$

The capacitor, *Cpi*, for the circuit is the PZT itself because, electrically, it behaves similar to a capacitor. The capacitance value of the circuit cannot be changed in order to tune the circuit at a desired resonant frequency unless a variable capacitor is added in parallel or in series. If the capacitance of the PZT has to be reduced, a variable capacitor can be added in series with the PZT. Alternatively, a variable capacitor can be added in parallel with the PZT to increase the capacitance. A simpler alternative is to use a variable inductor as the shunt inductor in order to tune the circuit. The inductance for the RLC circuit, L_s, was simulated with an operational amplifier circuit as shown in Figure 4 [20]. The resistor, R_2, is a variable resistor that can be adjusted in order to change the circuit inductance. The components labeled R_1, R_3, and R_4 are 10 kΩ resistors, and C_1 is a 10 000 μF capacitor.

5. SHUNT CIRCUIT TUNING

For tuning the shunted circuits, one needs to first determine the electrical frequencies required for dissipating energy at the mechanical resonance frequencies. The second step involves calculating the initial values for the variable resistors in the shunt circuit. The final step is fine-tuning the resistors through testing in order to achieve optimal damping.

An optimal electrical resonant frequency must be calculated because the electrical resonant frequency is not exactly the same as the resonant plate frequency due to inherent damping in the plate and added damping of the shunt circuit. An optimal tuning ratio, δ_{opt}, is calculated to determine the electrical resonant frequency of the circuit, ω_e.

Several experimental parameters, however, must be determined before δ_{opt} and ω_e can be calculated. These parameters include the natural frequencies of the plate when the PZTs are

in open- and short-circuit configuration, the generalized electromechanical coupling coefficient K_{31}, the optimal tuning inductance and capacitance, and the shunting resistance for each mode. It is difficult to determine these optimal tuning parameters using the conventional shunt circuit theories developed by many researchers for two main reasons. The first is that the PZT capacitance and the shunt inductance have some internal resistances and these are not negligible. The second is that the material parameters of capacitors (PZTs) used in the shunt electric circuit vary 5–10% from manufacturer's values.

First, the capacitance of the PZT should be determined roughly (since capacitance is dependent on frequency) using

$$C_p^T = \frac{K_3^T \times \varepsilon_0 \times A_p}{t_p}, \tag{2}$$

where C_p^T is the capacitance of the PZT at constant stress, K_3^T the relative dielectric constant at 1 kHz, the constant ε_0 is $8{\cdot}85 \times 10^{-12}$ F/m, A_p the surface area of PZT, and t_p the thickness of the PZT. These values were provided by the manufacturer, Piezo Systems, Inc. The product of $K_3^T \varepsilon_0$ is called the permittivity of the dielectric denoted ε. The PZT capacitance at constant strain, C_p^S, is obtained from the equation

$$C_p^S = C_p^T(1 - k_{31}^2), \tag{3}$$

which is dependent upon the electromechanical coupling coefficient, k_{31}, provided by the manufacturer.

Second, the generalized electromechanical coupling constant for a piezoelectric bonded to a structure can be obtained from the frequency change of the electric boundary conditions [5]:

$$K_{31}^2 = \frac{(\omega_n^D)^2 - (\omega_n^E)^2}{(\omega_n^E)^2}. \tag{4}$$

Here ω_n^D and ω_n^E are the natural frequencies of the structural mode of interest with an open-circuit piezoelectric and a short-circuit piezoelectric respectively. These frequencies can be obtained from the frequency response function. The other optimum tuning parameters are calculated from the values determined above as

$$\delta_{opt} = \sqrt{1 + K_1^2} \tag{5}$$

and

$$\omega_e = \delta_{opt} \omega_m, \tag{6}$$

where δ_{opt} is the optimal tuning ratio and ω_e the electrical resonant frequency.

The shunt inductance and PZT capacitance determine the electrical resonance of the circuit, according to

$$\omega_e = \frac{1}{\sqrt{_s C_p^S}}. \tag{7}$$

The shunt inductance, L_s, is calculated from ω_e and the PZT capacitance, C_p^S:

$$L_s = \frac{1}{\omega_e^2 C_p^S}. \tag{8}$$

The equivalent inductance of the op-amp circuit shown in Figure 4 is determined to be

$$L_{eq} = R^* C_1, \tag{9}$$

where

$$R^* = \frac{R_1 R_3 R_4}{R_2}. \tag{10}$$

The resistor, R_2, in the inductor circuit shown in Figure 4 is a variable resistor that is adjusted in order to change the circuit inductance.

For a desired inductance of L_s, the value of R_2 is determined from the equation

$$R_2 = \frac{R_1 R_3 R_4 C_1}{L_s}. \tag{11}$$

To determine the optimal shunt load resistance, R_L of Figure 4, the optimal damping ratio, r_{opt}, must be calculated using the value K_{31} from equation (5):

$$r_{opt} = \sqrt{2}\frac{K_{31}}{1 + K_{31}^2}. \tag{12}$$

The optimal shunt load resistance, R_{opt}, is then calculated as

$$R_{opt} = \frac{r_{opt}}{C_p^S \omega_n^E}. \tag{13}$$

The values for the inductor resistance and load resistance were calculated according to the above equations, and they were used for the initial tuning of the shunt circuits. The fine-tuning of the circuits was performed using preliminary tests that helped us determine the effectiveness of the initial tuning and the extent of further tuning needed.

Once the test plate was clamped into the test window, as shown in Figure 5, the PZT shunts were turned to the plate resonant frequencies. In order to set the shunt circuit inductors to the required values, the plate resonant frequencies were determined through a simplified modal test using an accelerometer and impact hammer. The accelerometer measurement was taken at the center of the plate, and the impact was applied to the center of the top third part of the plate. The shunt circuits were tuned in the test window to the plate frequencies.

As Figure 6 shows, a quick test of the shunt circuits indicates that they have been properly tuned, as the plate vibrations at the selected peaks are significantly lowered with the shunt circuits turned on. It is worth noting that the peak at 190 Hz was not selected because it represents an even mode of the plate that does not contribute to noise transmission as greatly as the other peaks that have been selected (i.e., those numbered as 1, 3, 4, and 5).

6. TRANSMISSION LOSS CALIBRATION TESTS

The transmission loss was calculated as

$$TL = MNR + 10\log_{10}(A/S\alpha), \tag{14}$$

where TL is the transmission loss of the panel, MNR the measured noise reduction between the reverberation room and reception chamber, $S\alpha$ the Sabine absorption of the receiving

Figure 5. Plate with electrically shunted PZTs in the (reception chamber side) modified test window of the transmission loss facility.

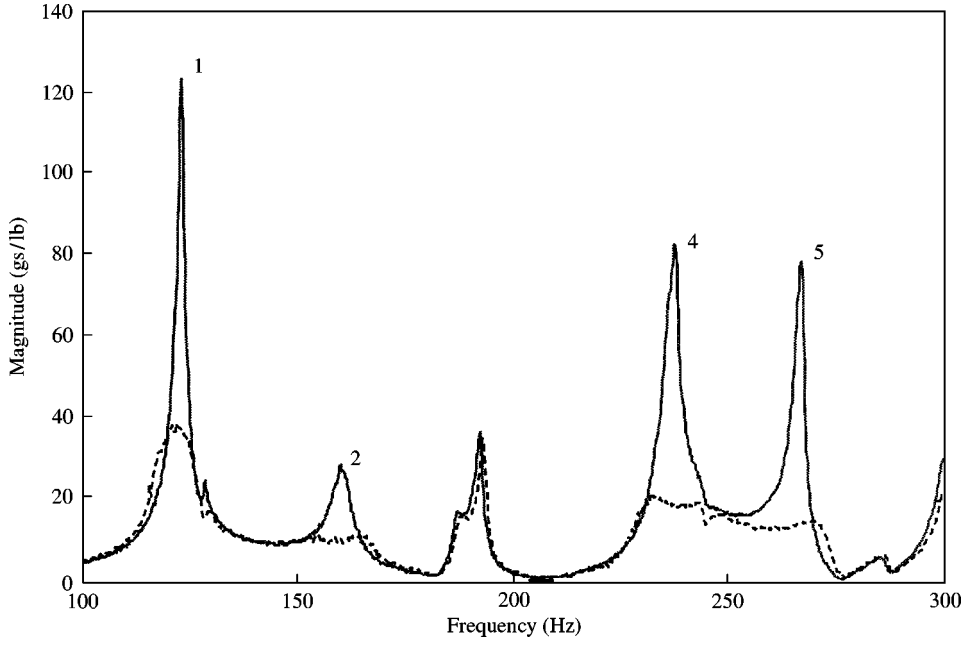

Figure 6. Vibration transfer functions (g's/lb) for a plate with electrically shunted PZTs (- - -) and a plate with unshunted PZTs (——).

room, and A the area of the test window. Since the expression $10\log_{10}(A/S\alpha)$ is constant for any test panel with the same area, equation (14) can be modified to

$$TL = MNR - CF, \tag{15}$$

where CF represents a constant correction factor. To determine the correction factor for our test window, a flexible test sample was made of 2 mm thick barrier material to clamp into the test window, as shown in Figure 2. The transmission loss of the barrier material from 100–10 000 Hz can be directly calculated from the mass-law equation

$$TL_{calc}(\text{dB}) = 20\log_{10} W + 20\log_{10} f - 47{\cdot}2, \tag{16}$$

where TL_{calc} is the theoretical transmission loss, W is the weight density of the panel, and f is the center frequency of the third-octave measurement band.

Using a white noise with a bandwidth of 100–10 000 Hz, we measured the noise level in the reverberation and the reception chambers in order to determine the measured noise reduction (MNR). The measured noise reduction was used to calculate the correction factor for each third octave band, according to

$$CF = MNR - TL_{calc}. \tag{17}$$

The transmission loss for the test plates was then calculated according to

$$TL_{std} = MNR_{std} - CF. \tag{18}$$

7. TRANSMISSION LOSS TEST RESULTS

After the shunt circuits were tuned, the transmission loss at a single frequency was tested to determine the effect of shunted PZTs. The sound pressure transmission for a single tone at 162·75 Hz (peak 3), generated by the speakers in the reverberation chamber, was measured in the reception room. As Figure 7 shows, the reception room sound transmission loss increased by approximately 5·8 dB when the shunt circuits were turned on.

The PZT plate was then tested with and without the shunt circuits, for a broadband input of 10–10 000 Hz, in order to further determine the effect of the shunted PZTs. As Figure 8 shows, a significant increase in sound transmission loss occurs in the frequency range of 100–300 Hz with the shunted PZTs. The effective range of the shunted PZTs is the same as the range for which they were tuned, as discussed earlier. The test results show that the shunted PZTs do not significantly affect sound transmission loss at frequencies higher than 300 Hz, which is outside of the range of the shunt circuit tuning. Figure 8 further shows that the shunted PZTs have the most significant effect on the 125 and 250 Hz third-octave bands; two of the frequencies that the shunt circuits were tuned to. For the 100–400 Hz frequency range, the plate with shunted PZTs has approximately 7 dB of higher transmission loss than an undamped plate.

The performance of shunted PZTs was further evaluated by comparing the shunted PZT plate with a plate with constrained layer damping. The constrained layer damping that was used for our study was MASDAMP 755, manufactured by Lear Corporation (a leading supplier of automotive damping materials). MASDAMP 755, which weighs approximately 4·89 kg/m^2 (1 lb/ft^2), is a widely used constrained layer damping material in the automotive industry. There was no attempt in this study to optimize the passive damping material for our test plate. We merely wanted to compare the sound transmission loss performance of

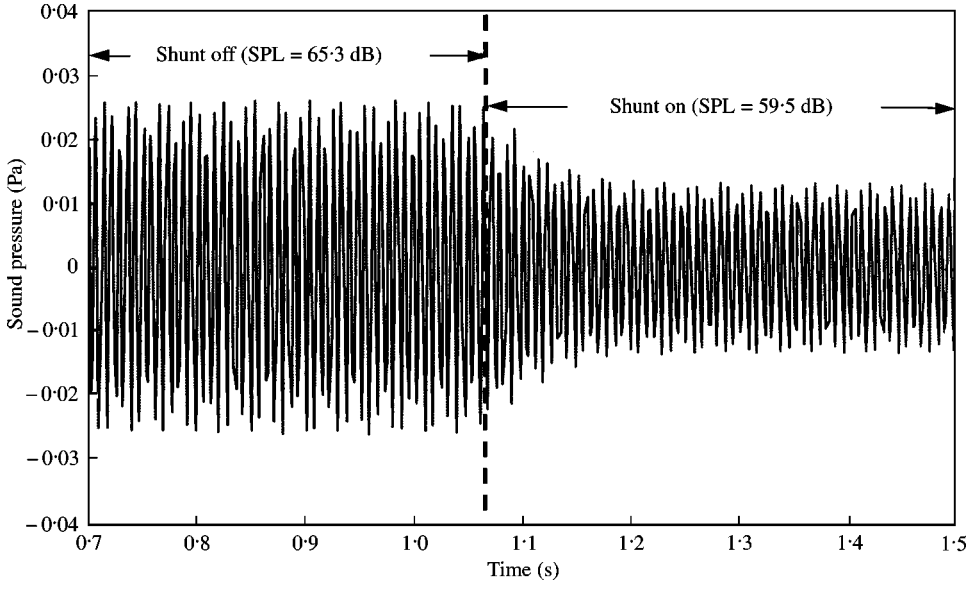

Figure 7. Effects of shunted PZTs on sound transmission loss at 162·75 Hz.

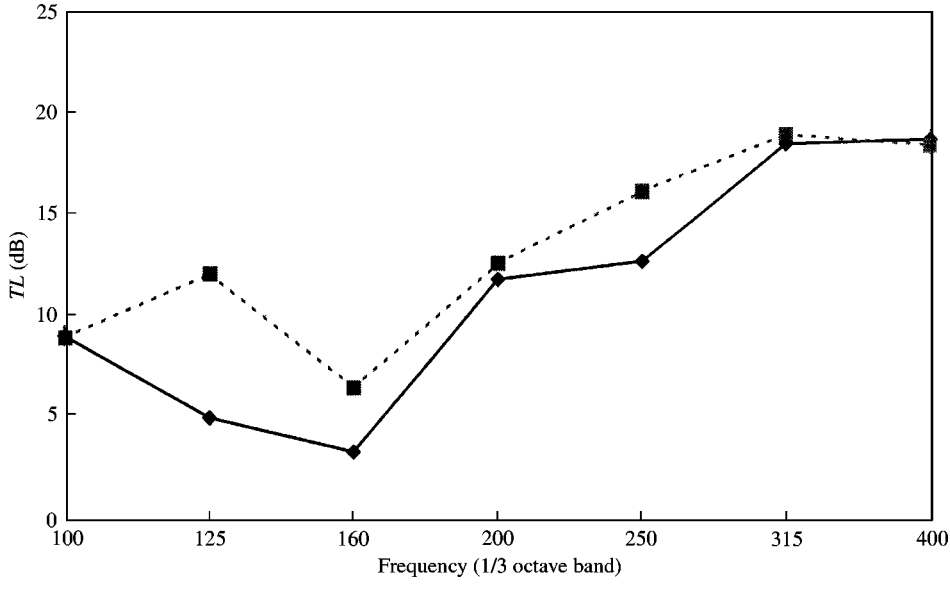

Figure 8. Transmission loss for test plate with unshunted plate (——) and shunted PZTs (- - -) in 100–400 Hz frequency range.

shunted PZTs with one of the commonly used, premium, passive damping materials; and the choice of MASDAMP 755 fits these criteria.

In order to provide a direct comparison between the damping effects of shunted PZTs with constrained layer damping, the transmission loss data for the damped plate was

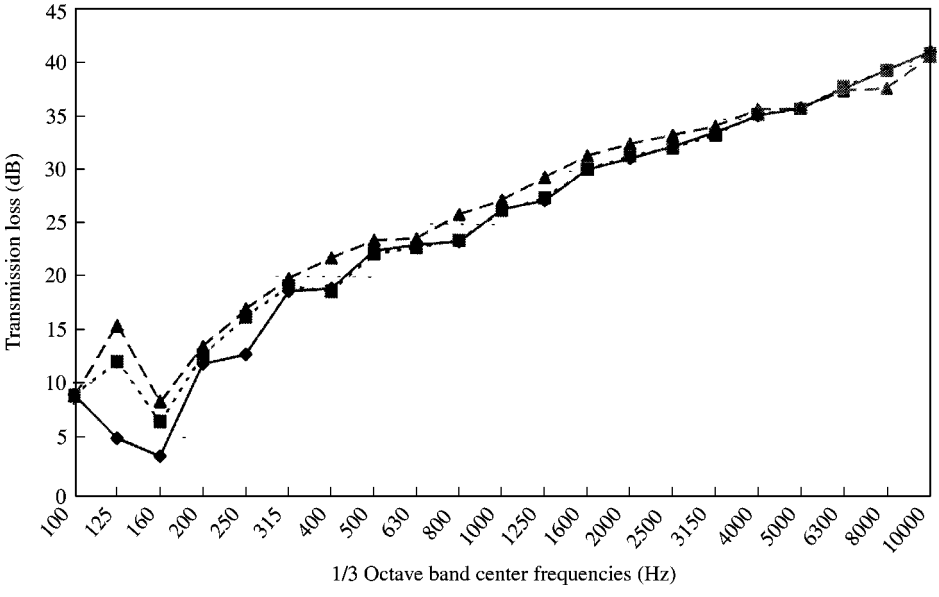

Figure 9. Transmission loss results for a plate with unshunted PZTs (- - -), Shunted PZTs (——), and constrained layer damping (– – –) in the frequency range of 100–1000 Hz.

adjusted to eliminate the mass loading effect of the damping material. From equation (16), the added transmission loss due to the weight of the panel is

$$TL_{mass} = 20 \log_{10} W. \tag{19}$$

For the PZT plate, with an area weight density of 7·413 kg/m^2, this mass-loading factor is

$$TL_{mass} = 17{\cdot}40 \text{ dB}. \tag{20}$$

For the damped plate, which has an area density of 9·600 kg/m^2, the mass-loading factor is

$$TL_{mass} = 19{\cdot}64 \text{ dB}. \tag{21}$$

Therefore, the additional transmission loss created by the mass of the constrained layer damping is 2·24 dB.

Figure 9 shows the transmission loss comparison between the three plates that were tested. It indicates that the constrained layer damping material can actually provide a larger transmission loss than shunted PZTs, but at the expense of adding much more weight to the structure. For many applications, however, the added weight due to the passive damping material may be unacceptable. For such applications, the shunted PZTs will provide the most significant benefits.

To further illustrate this point, we will analyze the benefits of the shunted PZTs and the constrained layer damping materials, as normalized with respect to the weight they add to the structure, i.e.,

$$\frac{\Delta(TransmissionLoss)}{\Delta(AddedWeight)} = \frac{\Delta(TL)}{\Delta W}, \tag{22}$$

where

$$\Delta(TL) = TL|_{treated\ plate} - TL|_{standard\ plate}, \qquad \Delta W = W|_{treated\ plate} - W|_{standard\ plate}. \tag{23, 24}$$

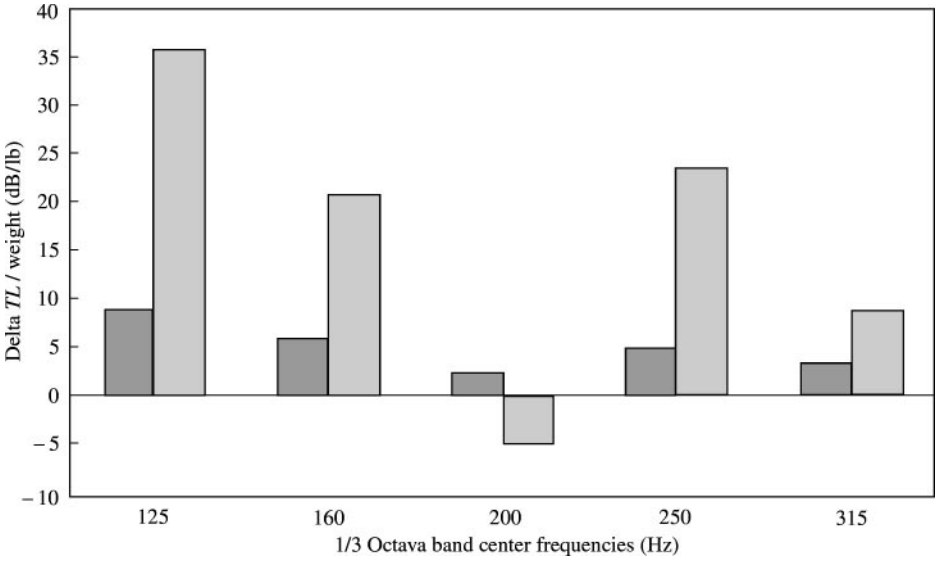

Figure 10. Increased transmission loss normalized with respect to added weight; ▭, for a plate with shunted PZTs; (■) for constrained layer damping.

As clearly shown in Figure 10, the shunted PZTs have a significantly larger transmission loss-to-weight ratio at all of the frequencies for which they are tuned (i.e., 125, 160, and 250 Hz) than the passive constrained layer damping treatments. The implication of the results in Figure 10 is that smart damping materials can be used for weight-sensitive applications to provide a higher transmission loss at selected frequencies without adding any significant amount of weight to the structure. It is worth noting that the results shown in Figure 10 do not include the weight of the shunt circuit electronics that was used for our laboratory experiments. This is because we believe that in the eventual application of the technology that is presented in this research, the shunt circuits are either embedded into the electronics that are already present in a typical vehicle or designed into an application-specific integrated circuit (ASIC), thus adding nearly no weight to the vehicle.

8. SUMMARY

The application of electrically shunted piezoceramic materials (PZTs) for increasing transmission loss is studied. Shunted PZTs were considered because they offer a simpler and more cost-effective alternative to actively controlled PZTs; therefore, making them more suitable for cost-sensitive applications. The test setup in a SAE J1400 test facility was described, followed by a detailed description of the shunt circuit and tuning procedure. Next, the effect of shunted PZTs on increasing sound transmission loss for a test plate with different damping conditions was presented.

The SAE J1400 test results indicated that shunted PZTs can increase sound transmission loss by approximately 6 dB for a pure tune input at 162 Hz, and 7 dB for a broad band input of 10–10 000 Hz. The test results further showed that constrained layer damping materials could provide a sound transmission loss that is comparable to PZTs, but at a substantially higher added weight. A comparison of the transmission loss-to-weight ratio

between PZTs and constrained layer damping materials indicated that PZTs are far more advantageous than constrained layer damping materials.

The results of this study extend the previously observed benefits of the PZTs for reducing structure-borne noise to increasing transmission loss in structures. Further, the results re-affirm the suitability of PZTs for weight-sensitive applications where the added weight due to passive damping treatments cannot be tolerated. For cost-sensitive applications with low concern for the added weight, however, passive-damping treatments may still prove to be most effective.

REFERENCES

1. N. W. HAGOOD and A. VON FLOTOW 1991 *Journal of Sound and Vibration* **146**, 243–268. Damping of structural vibrations with piezoelectric materials and passive electrical networks.
2. B. MULCAHEY and R. L. SPANGLER 1998 *Machine Design* **70**, 60–63. Peizos tame tough vibrations.
3. P. A. EISENSTEIN 1994 *Automotive Industries* **174**, 108–111. NVH: The new battleground.
4. Lord Corporation: http://www.lordtalent.com.
5. Encarta Concise Encyclopedia Online: http://encarta.msn.com.
6. *IEEE Standard on Piezoelectricity*: *Std* 176-1987 1988. New York: The Institute of Electrical and Electronics Engineers Inc.
7. Sensor Technology Limited: http://www.sensortech.ca/fig1-3.html.
8. 1998 *Machine Design* **70**, 46–47. Batter up! piezo dampers take sting out of swing.
9. J. Q. SUN, M. A. NORRIS, D. J. ROSSETTI and J. H. HIGHFILL 1996 *Transactions of the American Society of Mechanical Engineers Journal of Vibration and Acoustics* **118**, 676–681. Distributed piezoelectric actuators for shell interior noise.
10. W. SHIELDS, J. RO and A. BAZ 1997 *Proceedings of the SPIE—The International Society for Optical Engineering* **3039**, 70–90. Control of sound radiation from a plate into an acoustic cavity using active piezoelectric-damping composites.
11. V. V. VARADAN, Z. WU, S. Y. HONG and V. K. VARADAN *The Institute of Electrical and Electronics Engineers* 1991 *Ultrasonics Symposium Proceedings* **1386**, 991–994. Active control of sound radiation from a vibrating structure.
12. V. V. VARADAN, S. V. GOPINATHAN, LIM YOUNG HUN and V. K. VARADAN 1998 *Proceedings of the SPIE—The International Society for Optical Engineering* **3323**, 546–553. Radiated noise control via structural vibration control.
13. L. LECCE, F. FRANCO, B. MAJA, G. MONTOURI and N. C. ZANDONELLA 1995 28*th International Symposium on Automotive Technology and Automation*. Vibration active control inside a car by using piezo actuators and sensors.
14. K. K. HENRIOULLE, W. DEHANDSCHUTTER and P. SAS 1998 *Journal-A* **39**, 30–34. Increasing the sound transmission loss through a double panel partition using a distributed acoustic actuator.
15. B. XIAOQI, V. V. VARADAN and V. K. VARADAN 1995 *Smart Materials and Structures* **4**, 231–239. Active control of sound transmission through a plate using a piezoelectric actuator and sensor.
16. *SAE Standards*, Document Number J1400 1990. Laboratory measurements of the airborne sound barrier performance of automotive materials and assemblies.
17. K. M. JERIC 1999 *Master of Science Thesis*, Department of Mechanical Engineering, Virginia Tech., An experimental evaluation of the application of smart damping materials for reducing structural noise and vibrations.
18. M. AHMADIAN and K. M. JERIC 1999 *Proceedings of* 1999 *SAE Off-Highway Equipment Congress and Exposition*. The application of piezoceramics for reducing noise and vibrations in vehicle structures.
19. M. AHMADIAN, K. M. JERIC and D. J. INMAN 1999 *Proceedigns of* 1999 *American Society of Mechanical Engineers Design Engineering Technical Conference*. An experimental evaluation of smart damping materials for reducing structural noise and vibrations.
20. P. HOROWITZ and W. HILL 1989 *The Art of Electronics*. Cambridge: Cambridge University Press.